Journal of Microbiology (2022) Vol. 60, No. 7, pp. 668–677
DOI 10.1007/s12275-022-2089-9
eISSN 1976-3794
pISSN 1225-8873

Description of *Corynebacterium poyangense* sp. nov., isolated from the feces of the greater white-fronted geese (*Anser albifrons*)[§]

Qian Liu[1], Guoying Fan[2], Kui Wu[2], Xiangning Bai[1], Xi Yang[1], Wentao Song[2], Shengen Chen[2], Yanwen Xiong[1*], and Haiying Chen[2*]

[1]*State Key Laboratory of Infectious Disease Prevention and Control, National Institute for Communicable Disease Control and Prevention, Chinese Center for Disease Control and Prevention, Changping, Beijing 102206, P. R. China*
[2]*The Collaboration Unit for Field Epidemiology of State Key Laboratory of Infectious Disease Prevention and Control, Jiangxi Provincial Key Laboratory of Animal-origin and Vector-borne Diseases, Nanchang Center for Disease Control and Prevention, Nanchang 330038, P. R. China*

(Received Feb 25, 2022 / Revised Apr 20, 2022 / Accepted Apr 25, 2022)

Two novel Gram-positive, non-spore-forming, facultatively anaerobic, non-motile, and short rods to coccoid strains were isolated from the feces of the greater white-fronted geese (*Anser albifrons*) at Poyang Lake. The 16S rRNA gene sequences of strains 4H37-19^T and 3HC-13 shared highest identity to that of *Corynebacterium uropygiale* Iso10^T (97.8%). Phylogenetic and phylogenomic analyses indicated that strains 4H37-19^T and 3HC-13 formed an independent clade within genus *Corynebacterium* and clustered with *Corynebacterium uropygiale* Iso10^T. The average nucleotide identity and digital DNA-DNA hybridization value between strains 4H37-19^T and 3HC-13 and members within genus *Corynebacterium* were all below 95% and 70%, respectively. The genomic G + C content of strains 4H37-19^T and 3HC-13 was 52.5%. Diphosphatidylglycerol (DPG), phosphatidylglycerol (PG), phosphatidylinositol (PI), phosphatidylcholine, and phosphatidyl inositol mannosides (PIM) were the major polar lipids, with $C_{18:1}\omega9c$, $C_{16:0}$, and $C_{18:0}$ as the major fatty acids, and MK-8 (H_4), MK-8(H_2), and MK-9(H_2) as the predominant respiratory quinones. The major whole cell sugar was arabinose, and the cell wall included mycolic acids. The cell wall peptidoglycan contained *meso*-diaminopimelic acid (*meso*-DAP). The polyphasic taxonomic data shows that these two strains represent a novel species of the genus *Corynebacterium*, for which the name *Corynebacterium poyangense* sp. nov. is proposed. The type strain of *Corynebacterium poyangense* is 4H37-19^T (=GDMCC 1.1738^T = KACC 21671^T).

*For correspondence. (Y. Xiong) E-mail: xiongyanwen@icdc.cn / (H. Chen) E-mail: nccdcchy@126.com
[§]Supplemental material for this article may be found at https://doi.org/10.1007/s12275-022-2089-9.

Keywords: *Corynebacterium poyangense* sp. nov., feces, migratory bird, Poyang Lake, greater white-fronted geese

Introduction

Corynebacterium is the type genus of the family *Corynebacteriaceae*, order *Corynebacteriales*, class *Actinomycetia*, phylum *Actinomycetota* (Ludwig *et al.*, 2015; Salam *et al.*, 2020; Oren and Garrity, 2021). The genus *Corynebacterium* is composed of Gram-positive, non-motile, non-spore-forming, rod- or club-shaped, catalase-positive bacteria with a high G + C content (Bernard and Funke, 2015; Nouioui *et al.*, 2018). As of 21 February 2022, the genus *Corynebacterium* included 136 species with validly published and correct names (https://lpsn.dsmz.de/genus/corynebacterium) (Parte *et al.*, 2020). Species of *Corynebacterium* have been recovered from a variety of samples, such as humans, animals, soil, water, and food (Bernard and Funke, 2015). The type species, *Corynebacterium diphtheriae*, is a well-known human pathogen that causes diphtheria by multiplying and secreting diphtheria toxin (Sharma *et al.*, 2019). However, *Corynebacterium glutamicum*, a non-pathogenic species, is commonly used as biochemical industrial producers of amino acids (Yu *et al.*, 2021).

The greater white-fronted geese (*Anser albifrons*) belong to migratory birds which hold long-distance migration every year and might spread emerging and re-emerging pathogens across the world (Samuel *et al.*, 2005; Boros *et al.*, 2018; Xiang *et al.*, 2019; Fukuda *et al.*, 2021; Zhu *et al.*, 2021). In the previous study, a novel bacterial genus (*Nanchangia*) and two novel species of genus *Corynebacterium*, i.e., *C. anserum*, and *C. heidelbergense*, were identified from feces of migratory birds (Braun *et al.*, 2018; Liu *et al.*, 2021a, 2021b). In this study, we isolated two strains 4H37-19^T and 3HC-13, belonging to undescribed species within the genus *Corynebacterium*, from the feces of the greater white-fronted geese, and depicted the taxonomic characteristics of the two strains.

Materials and Methods

Bacterial isolation and deposition

Fecal samples of the greater white-fronted geese (*Anser albifrons*) were obtained from Poyang Lake in China. The specimens were homogenized and serially diluted (10^{-4}–10^{-1}) in sterile phosphate-buffered saline. The diluted samples were spread on tryptone soya agar (TSA) and incubated at 37°C. Pure colonies were obtained by repeated subcultivations and stored at -80°C in 30% (v/v) glycerol stocks for further identification. The representative isolates were deposited at Guangdong Microbial Culture Collection Center (GDMCC) of China and Korean Agricultural Culture Collection (KACC) under the accession numbers GDMCC 1.1738 and KACC 21671, respectively.

Phylogenetic analyses

For phylogenetic analyses, 16S rRNA gene sequences of strains 4H37-19^T and 3HC-13 were amplified using primers 27F and 1492R, and then sequenced through the Sanger sequencing (Zhu *et al.*, 2022). The obtained sequences were searched against the quality-controlled databases of 16S rRNA sequences using EzBioCloud service (Yoon *et al.*, 2017). Phylogenetic trees were constructed using the MEGA-X program based on neighbor-joining (NJ), maximum-likelihood (ML), and minimum-evolution (ME) algorithms with 1,000 bootstrap replicates (Kumar *et al.*, 2018). *Mycobacterium tuberculosis* H37Rv^T was used as the outgroup.

Whole-genome sequence analyses

Genomic DNA was extracted from pure culture using the Wizard Genomic DNA Purification kit (Promega). To obtain the complete genome of strain 4H37-19^T, a combination of PacBio Sequel platform and Illumina NovaSeq platform was used. The draft genome of strain 3HC-13 and *C. uropygiale* Iso10^T were sequenced on the Illumina NovaSeq platform. After filtering out the low-quality reads, the SPAdes optimizer Unicycler v0.4.8 (Wick *et al.*, 2017) was used for *de novo* assembly. Multiple rounds of polishing were performed with Pilon 1.23 (Walker *et al.*, 2014) in the Unicycler pipeline to correct small sequence errors. To further validate the taxonomic status of the two strains in the genus *Corynebacterium*, up-to-date bacterial core gene (UBCG, https://www.ezbiocloud.net/tools/ubcg) trees (Na *et al.*, 2018; Kim *et al.*, 2021) were constructed using the FastTree program with *Mycobacterium tuberculosis* H37Rv^T as the outgroup (Price *et al.*, 2010). To evaluate the genomic relatedness, the digital DNA–DNA hybridization (dDDH) values and average nucleotide identity (ANI) values were calculated using the Genome-to-Genome Distance Calculator (GGDC) 2.1 (http://ggdc.dsmz.de/) (Meier-Kolthoff *et al.*, 2022) and OrthoANI tool (Lee *et al.*, 2016; Yoon *et al.*, 2017), respectively. Gene annotation was performed using NCBI Prokaryotic Genome Annotation Pipeline (PGAP) (Li *et al.*, 2021) and Rapid Annotation using Subsystem Technology (RAST) server (https://rast.nmpdr.org/) (Brettin *et al.*, 2015). The secondary metabolite biosynthesis gene clusters were predicted using antiSMASH 6.0 (Blin *et al.*, 2021). Carbohydrate-active enzyme features were analyzed in the dbCAN2 meta server, using DIAMOND, HMMER and eCAMI tools, respectively (https://bcb.unl.edu/dbCAN2/index.php) (Yin *et al.*, 2012; Zhang *et al.*, 2018).

Comparative analyses

Based on the 16S rRNA gene similarities, the four closely related type strains (*C. uropygiale* Iso10^T, *C. choanae* 200CH^T, *C. jeikeium* NCTC 11913^T, and *C. falsenii* DSM 44353^T) purchased from three culture collections (JCM, ATCC, and CCUG) were used as the reference strains for phenotypic, biochemical, and chemotaxonomic comparisons with strains 4H37-19^T and 3HC-13. Comparative genome analyses and pairwise comparisons of ANI and dDDH values were also performed with genomic data of representative strains within the genus *Corynebacterium* publicly available from NCBI database. Whole-genome orthologous gene annotations and comparisons, including the genetic ontogeny of all predicted protein-coding genes, were conducted using OrthoVenn2 (Xu *et al.*, 2019).

Growth conditions and morphological characterization

To determine the optimal growth conditions, strains 4H37-19^T and 3HC-13 were cultured under various conditions. The growth temperatures were tested in tryptone soya broth (TSB) at 4, 10, 15, 20, 25, 30, 37, 45, 50, and 55°C, respectively. The salt tolerance was determined by culturing strains 4H37-19^T and 3HC-13 in the presence of different NaCl concentrations (0, 0.5, 1, 1.5, 2, 3, 4, 5, 6, 7, 8, 10, and 12%, w/vol) in TSB. Growth was also evaluated at different pH values (4.0–11.0, at 1.0 pH unit intervals) using TSB. The pH values were re-adjusted after sterilization (121°C, 15 min) if necessary. The optimal growth conditions were determined by measuring the turbidity at 600 nm using Varian Cary 50 spectrophotometer (CARY-50, Agilent Technologies). The cells cultured under optimum conditions in TSB was used for following analyses, unless otherwise mentioned. Oxygen tolerance was evaluated in an anaerobic chamber in the presence of N_2 (90%), H_2 (5%), and CO_2 (5%) for 1 week. Cell morphologies were observed under a transmission electron microscope (HT7700, Hitachi). Gram staining reactions and spore formation were observed under a light microscope (Eclipse 50i, Nikon) using a Gram staining kit (bioMérieux) and the malachite green staining method (Schaeffer and Fulton, 1933). Semi-solid medium containing 0.4% agar was used for motility testing. Catalase and oxidase activity were detected as previously described (Liu *et al.*, 2021a). Antibiotic resistance was determined using K-B method (Bauer *et al.*, 1966).

Biochemical and chemotaxonomic analyses

The biochemical characteristics of strains 4H37-19^T and 3HC-13 were tested using API 50 CH (combined with API 50 CHB/E), the API ZYM system and API Coryne kits following the manufacturer's instructions (bioMérieux). Cellular fatty acids of strains 4H37-19^T and 3HC-13, and four reference strains were extracted, analyzed, and identified according to the previous studies (Sasser, 1990; Kim *et al.*, 2021). The respiratory quinones of strain 4H37-19^T was extracted and analyzed by HPLC as previously reported (Collins *et al.*, 1977; Oh *et al.*, 2020). The polar lipids of the isolate was analyzed by two-dimensional thin-layer chromatography (TLC) as previously described by Minnikin *et al.* (1984). Whole-cell sugars were obtained by hydrolyzing the cell harvests in 0.5 M sulfuric acid (100°C, 2 h), as described previously (Komagata and Suzuki, 1988). The cell wall peptidoglycan was analyzed as described previously (Schumann, 2011). The mycolic acids were extracted as previously described (Guerrant *et al.*, 1981), then detected by gas chromatograph (HP 6890, Agilent) using an Ultra-2 chromatographic column (25 m by 0.2 mm inside diameter and 0.33 μm liquid film thickness). The temperature of the injector and detector were 250°C and 300°C, respectively. The flow rate of the carrier gas (hydrogen) was 300 ml/min.

Accession numbers

The DDBJ/ENA/GenBank accession numbers for the 16S rRNA gene sequences of strains 4H37-19^T and 3HC-13 are MN611115 and MN611764, respectively. The DDBJ/ENA/GenBank accession numbers for the whole-genome sequences of strain 4H37-19^T, strain 3HC-13 and *C. uropygiale* Iso10^T are CP046884, WWCB00000000, and JAKGSI000000000, respectively.

Results and Discussion

Phylogenetic and phylogenomic analyses

Based on almost full-length 16S rRNA gene sequences comparisons against the EzBioCloud database, strains 4H37-19^T and 3HC-13 were identified to be members of the genus *Corynebacterium* within family *Corynebacteriaceae*, and most

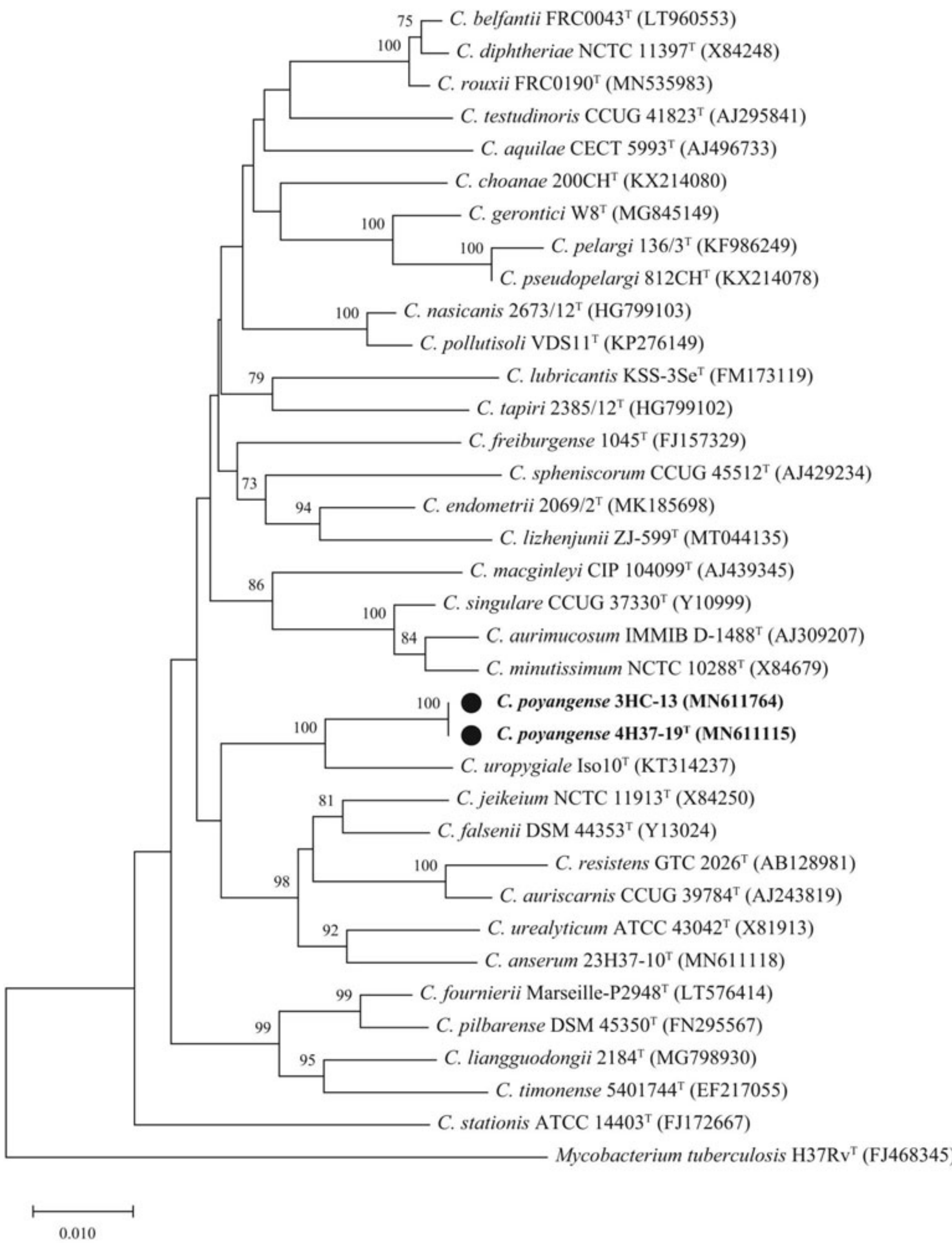

Fig. 1. The neighbor-joining phylogenetic tree based on 16S rRNA gene sequences of strain 4H37-19^T, strain 3HC-13, and closely related species. Bootstrap values (> 70%) based on 1,000 replicates are shown at branch nodes, with *Mycobacterium tuberculosis* H37Rv^T as an outgroup. Bar, 0.01 changes per nucleotide position. Strains from this study are highlighted in bold type and black circle.

Table 1. The genomic features of strain 4H37-19ᵀ, strain 3HC-13, and phylogenetically related species
Strains: 1, strain 4H37-19ᵀ (CP046884); 2, strain 3HC-13 (WWCB00000000); 3, *C. uropygiale* Iso10ᵀ (JAKGSI000000000); 4, *C. choanae* 200CHᵀ (CP033896); 5, *C. jeikeium* NCTC 11913ᵀ (UFXO00000000); 6, *C. falsenii* DSM 44353ᵀ (CP007156).

Characteristics	1	2	3	4	5	6
Size	2,617,997	2,559,826	2,460,278	2,986,773	2,526,027	2,719,616
Contigs	1	9	10	1	2	2
N50	2,617,997	828,747	515,070	2,986,773	2,516,825	2,677,607
Number of genes	2,465	2,386	2,293	2,141	2,262	2,401
Number of CDSs	2,401	2,331	2.235	2,075	2,200	2,306
G + C content (%)	52.5	52.5	66.2	57.04	61.43	63.15
rRNA genes (5S/16S/23S)	12 (4, 4, 4)	3 (1, 1, 1)	3 (1, 1, 1)	12 (4, 4, 4)	9 (3, 3, 3)	9 (3, 3, 3)
tRNA genes	49	49	52	51	50	50
ncRNA genes	3	3	3	3	3	1
Pseudo genes	43	37	23	28	50	35
CRISPR count	1	1	0	2	1	1

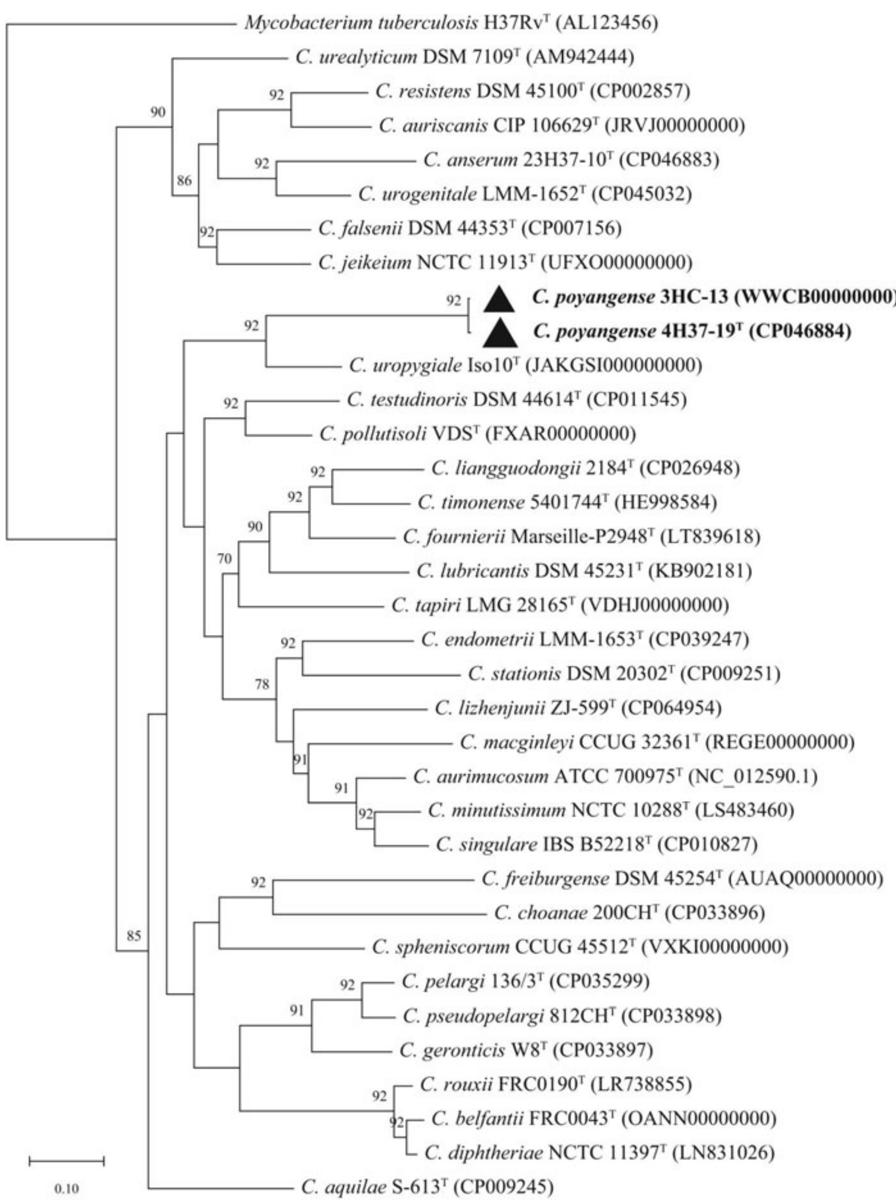

Fig. 2. The UBCG tree of strain 4H37-19ᵀ, strain 3HC-13, and phylogenetically related strains. Gene Support Index (GSI) presented (> 70%) on nodes are the numbers of single gene trees supporting the branch. *Mycobacterium tuberculosis* H37Rvᵀ was used as an outgroup. Bar, 0.10 substitutions per nucleotide. Strains from this study are highlighted in bold type and black triangle.

Table 2. Digital DNA-DNA hybridization (dDDH) and average nucleotide identity (ANI) values between genomes of the isolates and genomes of related strains

Strains	Accession numbers	dDDH (%)		ANI (%)	
		4H37-19^T	3HC-13	4H37-19^T	3HC-13
C. poyangense 4H37-19^T	CP046884	100.0	95.5	100.0	99.4
C. poyangense 3HC-13	WWCB00000000	95.5	100.0	99.4	100.0
C. choanae 200CH^T	CP033896	27.3	25.9	68.5	68.7
C. falsenii DSM 44353^T	CP007156	24.7	23.8	68.3	68.2
C. jeikeium NCTC 11913^T	UFXO00000000	26.6	25.0	68.2	67.8
C. urealyticum DSM 7109^T	AM942444	23.3	22.0	68.8	67.7
C. uropygiale JCM 32435^T	JAKGSI000000000	18.5	18.1	70.6	70.8

closely related to *C. uropygiale* Iso10^T (97.8% 16S rRNA gene identity), *C. choanae* 200CH^T (96.0%), *C. jeikeium* NCTC 11913^T (96.0%), *C. falsenii* DSM 44353^T (96.0%) and *C. urealyticum* DSM 7109^T (95.7%). These values were lower than 98.7%, the generally accepted threshold value for novel species (Rossi-Tamisier *et al.*, 2015), suggesting that the two isolates could represent a novel species of the genus *Corynebacterium*. In addition, the phylogenetic tree based on 16S rRNA gene sequences showed that strains 4H37-19^T and 3HC-13 formed a single clade and clustered with *C. uropygiale* Iso10^T (Fig. 1; Supplementary data Figs. S1 and S2).

Whole-genome analyses showed that strains 4H37-19^T and 3HC-13 contained 2,617,997 bp with a 52.5% DNA G + C content, and 2,559,826 bp with a 52.5% DNA G + C content, respectively. The genome of strain 4H37-19^T contained 2,465 genes and 2,401 CDSs, which were different with the number of genes 2,386 and CDSs 2,331 of strain 3HC-13 genome. To compare strain 4H37-19^T with strain 3HC-13 in detail, the conservation and variation were compared using MAUVE software (Darling *et al.*, 2011) with strain 4H37-19^T as the reference (Supplementary data Fig. S3). Result showed that these two genomes have a high content of homologous regions, including a total of 11 locally collinear blocks (LCBs) with minimum weight of 2,881 were generated. A total of 13,460 SNPs were located within genomes, and some regions of strain 3HC-13 displays inversion, translocation, and Tran+Inver, revealing different syntenial relationships to type strain 4H37-19^T. Strains 4H37-19^T and 3HC-13 may have the same genes related to the physiological and fatty acid characteristics. However, MAUVE result confirmed that genome of strains 4H37-19^T was different from that of strain 3HC-13. It also should be noted that genome of strain 4H37-19^T was a complete genome, but genome of strain 3HC-13 was a draft genome. (Supplementary data Fig. S3)

The genomic characteristics of the two isolates were compared with their closely related type species (Table 1). Compared with these four related species, strains 4H37-19^T and 3HC-13 had medium genome sizes, lower GC content genomes, and less number of tRNA genes.

To infer the UBCG tree, 92 housekeeping core genes of our isolates and their related type strains were extracted and concatenated. Phylogenomic result (Fig. 2) showed that strains 4H37-19^T and 3HC-13 clustered closely with *C. uropygiale* Iso10^T, consistent with result based on 16S rRNA gene sequences (Fig. 1). To determine the genome relatedness, dDDH and ANI values between our isolates and the closely related species of genus *Corynebacterium* were calculated and presented in Table 2. These values were below the threshold values for species demarcation (70% for dDDH value and 95–96% for ANI value) (Luo *et al.*, 2014; Chun *et al.*, 2018). Thus, the two isolates 4H37-19^T and 3HC-13 belonged to different species from these reference strains (Jackman *et al.*, 1987; Sjöden *et al.*, 1998; Braun *et al.*, 2016; Busse *et al.*, 2019). The dDDH and ANI values between stains 4H37-19^T and 3HC-13 were 95.5% and 99.4%, indicating that the two isolates belonged to the same species.

Genome and pangenome analyses

Using the RAST server, the genome of strain 4H37-10^T was annotated, 731 genes (29%) were further clustered into 24 subsystems. The most represented subsystem features were carbohydrates (201), amino acids and derivatives (193), protein metabolism (166), cofactors, vitamins, prosthetic groups, pigments (100), nucleosides and nucleotides (61), and DNA metabolism (46) (Fig. 3A). Screening the genes coding secondary metabolites showed that genome of strain 4H37-10^T contained four (Regions 1–4) different genes clusters of secondary metabolites (Fig. 3B). Region 1 (649,498–670,421 nt, total 20,924 nt) and region 2 (2,183,106–2,193,576 nt, total 10,471 nt) displayed terpene and an unspecified ribosomally synthesised and post-translationally modified peptide product (RiPP) cluster types, respectively. Both region 1 and 2 were unable to identify the most similar known gene cluster. Region 3 (2,247,432–2,281,292 nt, total 33,861 nt) and region 4 (2,436,578–2,481,374 nt, total 44,797 nt) showed 5% and 8% similarity to pyrrolomycin A/pyrrolomycin B/pyrrolomycin C/pyrrolomycin D genes (BGC0000130) and stambomycin A / stambomycin B / stambomycin C / stambomycin D genes (BGC0000151), respectively.

The OrthoVenn2 analysis assigned 2,358 protein sequences from strain 4H37-19^T to 2,255 orthologous clusters with 90 singletons, while 2,294 proteins from strain 3HC-13 were assigned to 2,234 clusters with 55 singletons. The Venn diagram (Supplementary data Fig. S4) showed 1,076 gene clusters shared by strains 4H37-19^T and 3HC-13, and their closely related type strains. In addition, the six strains had 91 unique gene clusters, with strains 4H37-19^T and 3HC-13 having two and zero unique gene cluster, respectively.

According to the results from dbCAN2 meta server, we identified a total of 88 genes encoding glycosil transferases (GT), 75 genes encoding glycosil hydrolases (GH), 22 genes encoding carbohydrate esterase (CE), 12 genes encoding carbohydrate-binding module (CBM), and 2 genes encoding auxiliary activities (AA) (Supplementary data Table S1).

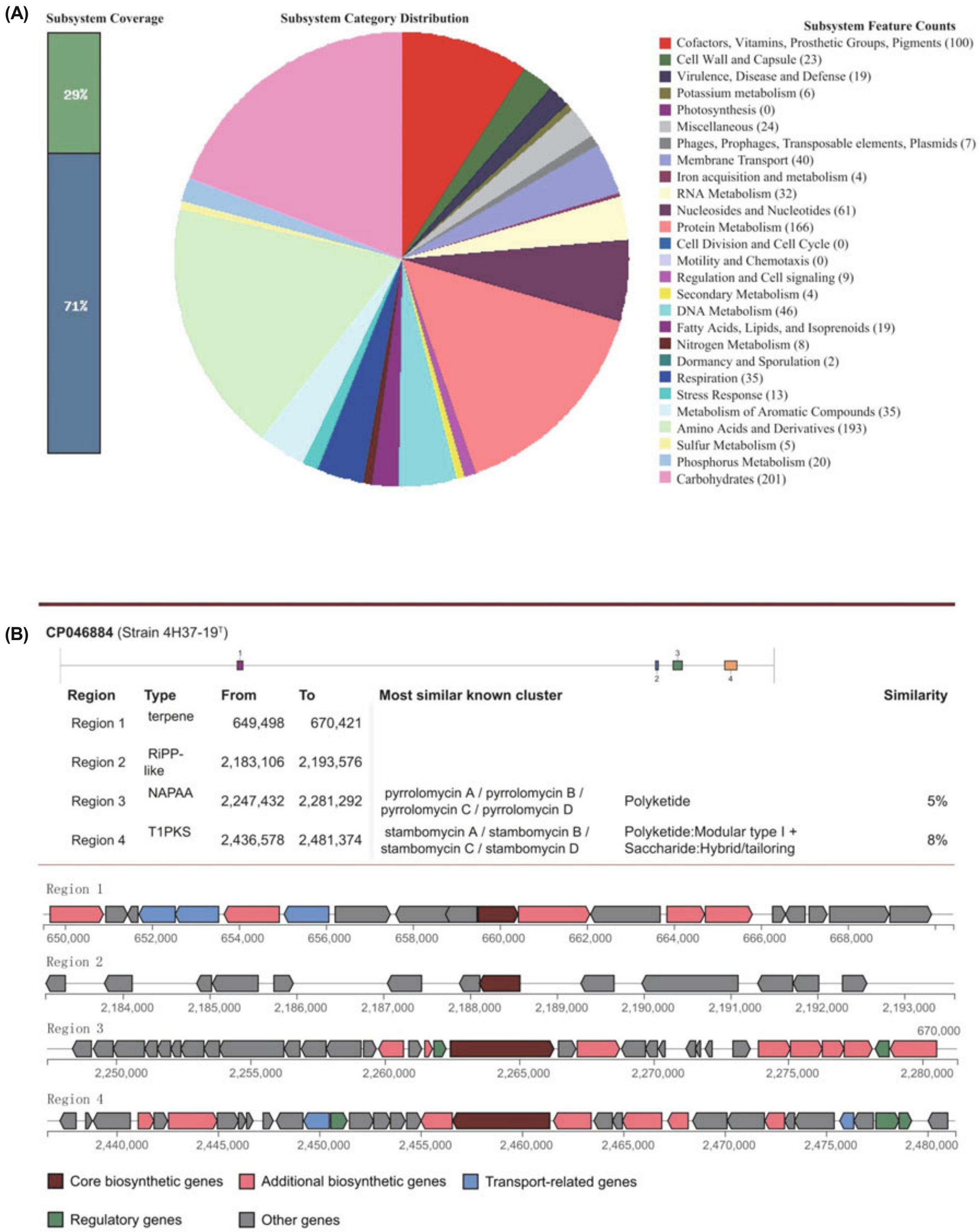

Fig. 3. Subsystems and secondary metabolism analyses in the genome of strain 4H37-19^T. (A) Annotated genome information using RAST server. (B) The secondary metabolite gene clusters predicted by antiSMASH 6.0.

Physiological, morphological, and biochemical features

Strains 4H37-19^T and 3HC-13 were Gram-stain-positive, facultatively anaerobic, non-motile and short rods to coccoid ($0.2–0.4 \times 0.6–0.9$ μm; Supplementary data Fig. S5). Cells were catalase-positive and oxidase-negative. Colonies were creamy whitish, circular colonies with rough edges on TSA. Strains 4H37-19^T and 3HC-13 grew at 15–45°C, pH 6.0–9.0 and in the presence of 0–7.5% (w/vol) NaCl in TSB, with optimal growth at 37°C, pH 7.0 and in the presence of 0.5–1.5% (w/vol) NaCl. Antibiotic testing indicated that strains 4H37-19^T and 3HC-13 were susceptible to amikacin, ampicillin, cefazolin, chloramphenicol, ciprofloxacin, clindamycin, erythromycin, gentamicin, kanamycin, penicillin G, streptomycin, sulfanilamide, tetracycline, and vancomycin.

The detailed biochemical characteristics of our isolates were described in the species descriptions, and the differential characteristics between strains 4H37-19^T and 3HC-13 and their closely related *Corynebacterium* type strains were summarized in Table 3. The cell morphology of strains 4H37-19^T and 3HC-13 were short rods to coccoid which were different with rod-club shape of *C. uropygiale* Iso10^T, *C. jeikeium* NCTC 11913^T, and *C. falsenii* DSM 44353^T, coccoid or irregular rod shape of *C. choanae* 200CH^T. Strains 4H37-10^T and 3HC-13, *C. uropygiale* Iso10^T, *C. jeikeium* NCTC 11913^T, and *C. falsenii* DSM 44353^T were non-spore-forming strains, except that *C. choanae* 200CH^T was not determined (Table 3). Biochemical results indicated that strains 4H37-19^T and 3HC-13 differed from their closely related neighbors by being positive for arbutin, L-arabinose, trypsin, α-glucosidase, and β-glucuronidase (Table 3). Strains 4H37-19^T and 3HC-13, *C. jeikeium* NCTC 11913^T, and *C. falsenii* DSM 44353^T were positive for alkaline phosphatase, while other related strains were negative. *Corynebacterium uropygiale* Iso10^T and *C. choanae* 200CH^T were positive for the reduction of nitrates, while the other related strains were negative, including our two isolates in this study. Furthermore, strains 4H37-19^T and 3HC-13, and *C. uropygiale* Iso10^T could utilize D-fructose, while the other related strains couldn't. *Corynebacterium choanae* 200CH^T, *C. jeikeium* NCTC 11913^T (weakly), and *C. falsenii* DSM 44353^T were positive for galactose, while our isolates and *C. uropygiale* Iso10^T were negative for this sugar.

Chemotaxonomic characteristics

The detailed fatty acid profiles of our isolates and their closely related type strains were showed in Table 3. The major fatty acids (> 10%) of strains 4H37-19^T and 3HC-13 were $C_{18:1}\omega9c$ (both were 53.4%), $C_{16:0}$ (22.8% and 22.9%, respectively), and $C_{18:0}$ (20.8% and 20.4%, respectively) (Table 4). Strain 4H37-19^T contained MK-8 (H_4) (38.3%), MK-8(H_2) (36.4%), and MK-9(H_2) (11.7%) as major respiratory quinones, which possessed the unique MK-8 (H_4) that was absent in their closely related type strains, such as *C. choanae* 200CH^T, and revealed different proportions of MK-8(H_2) and MK-9(H_2). (Bernard and Funke, 2015; Busse *et al.*, 2019). The polar lipid profile of strain 4H37-19^T was composed of diphosphatidylglycerol (DPG), phosphatidylglycerol (PG), phosphatidylinositol (PI), phosphatidylcholine (PC), phosphatidylinositol mannosides (PIM), two unidentified phospholipids (PL), and two unidentified glycolipids (GL) (Supplementary data Fig. S6), which was similar to those of their closely related strains (Bernard and Funke, 2015). The whole-cell sugar of strain 4H37-19^T consisted of arabinose (Supplementary data Fig. S7). The strain 4H37-19^T included mycolic acids in cell wall

Table 3. The differential characteristics of strain 4H37-19^T, strain 3HC-13 and type strains of reference species
Strains: 1, strain 4H37-19^T; 2, strain 3HC-13; 3, *C. uropygiale* Iso10^T; 4, *C. choanae* 200CH^T; 5, *C. jeikeium* NCTC 11913^T; 6, *C. falsenii* DSM 44353^T. +, positive; -, negative; W, weakly positive; A, aerobic; F, facultatively anaerobic; ND, not determined.

Characteristics	1	2	3	4*	5	6
Cell morphology	short rods to coccoid	short rods to coccoid	club shaped rods	coccoid or irregular rods	club-shaped rods	club-shaped rods
Spore forming	-	-	-	ND	-	-
Oxygen tolerance	FA	FA	FA	A	A	FA
Colony sizes	1–2 mm	1–2 mm	1–2 mm	0.5 mm	1–2 mm	< 2 mm
Colony color	creamy whitish	creamy whitish	creamy	creamy whitish	greyish-white	whitish
Enzyme activities						
Alkaline phosphatase	+	+	-	-	+	+
Leucine arylamidase	-	-	+	-	-	+
Lipase(C14)	w	-	-	-	-	+
Pyrazinamidase	-	-	-	-	-	+
Reduction of nitrates	-	-	+	+	-	-
Urease	-	-	-	-	-	+
Valine arylamidase	-	-	w	-	-	-
Trypsin	+	+	-	-	-	-
α-Glucosidase	+	+	-	-	-	-
β-Galactosidase	+	+	-	+	-	-
β-Glucosidase	+	+	-	+	-	-
β-Glucuronidase	+	+	-	-	-	-
Fermentation of						
Arbutin	+	+	-	-	-	-
D-Fructose	+	+	+	-	-	-
D-Galactose	-	-	-	+	w	+
D-Maltose	+	+	w	+	-	-
D-Mannose	+	+	+	+	-	-
D-Trehalose	+	+	-	+	-	-
L-Arabinose	+	+	-	-	-	-
Surcose	+	+	+	+	-	-

*Data from Busse *et al.* (2019).

Table 4. Composition of cellular fatty acids (%) of strain 4H37-19^T, strain 3HC-13 and the closely related species

Strains: 1, strain 4H37-19^T; 2, strain 3HC-13; 3, *C. uropygiale* Iso10^T; 4, *C. choanae* 200CH^T; 5, *C. jeikeium* NCTC 11913^T; 6, *C. falsenii* DSM 44353^T. TR, trace (< 0.5%); –, not detected.

	1	2	3	4*	5	6
Saturated straight chain						
$C_{12:0}$	-	-	TR	-	-	-
$C_{14:0}$	TR	TR	1.1	-	1.4	0.6
$C_{15:0}$	-	-	-	-	1.3	0.7
$C_{16:0}$	22.8	22.9	23.2	41.5	34.3	30.9
$C_{17:0}$	-	-	2.5	-	3.8	-
$C_{18:0}$	20.8	20.4	19.8	6.7	10.5	11.8
$C_{20:0}$	1.6	1.8	-	-	TR	-
Saturated branched chain						
iso-$C_{16:0}$	-	-	1.5	-	TR	-
iso-$C_{17:0}$	-	-	-	-	TR	-
iso-$C_{18:0}$	-	-	-	-	TR	0.5
iso-$C_{19:0}$	-	-	1.4	-	-	-
iso-$C_{20:0}$	-	-	-	-	TR	-
anteiso-$C_{15:0}$	-	-	-	-	TR	-
anteiso-$C_{17:0}$	-	-	0.7	-	0.5	-
$C_{18:0}$ 10-methyl	0.5	0.5	-	-	-	-
Unsaturated straight chain						
$C_{16:1}\omega9c$	-	-	-	-	-	1.6
$C_{17:1}\omega8c$	-	-	1.3	-	1.4	-
$C_{17:1}\omega5c$	-	-	1.2	-	-	-
$C_{18:1}\omega9c$	53.4	53.4	35.2	51.8	21.8	51.0
$C_{20:1}\omega9c$	-	-	-	-	TR	TR
$C_{20:4}\omega6,9c$	-	-	-	-	0.8	TR
Unsaturated branched chain						
$C_{14:0}$ 2OH	-	-	-	-	TR	-
$C_{16:0}$ 2OH	-	-	-	-	TR	-
$C_{17:0}$ 2OH	-	-	-	-	0.8	-
$C_{16:0}$ 3OH	-	-	-	-	TR	-
$C_{17:0}$ 3OH	-	-	-	-	-	TR
iso-$C_{19:1}$ I	-	-	-	-	TR	0.6
Summed features†						
3	-	-	6.7	-	1.2	TR
4	-	-	0.8	-	0.7	-
5	-	-	-	-	12.9	-
7	0.7	0.7	-	-	-	0.9
8	-	-	4.1	-	5.1	-

*Data from Busse *et al.* (2019).
†Summed features were used when two or three fatty acids could not be separated using the Microbial Identification System. Summed feature 3 was comprised of $C_{16:1}\omega7c$ and $C_{16:1}\omega6c$. Summed feature 8 was comprised of $C_{18:1}\omega7c$ and/or $C_{18:1}\omega6c$.

and contained *meso*-diaminopimelic acid (*meso*-DAP) in the peptidoglycan.

Taxonomic conclusion

Taken together, the overall phylogenetic, genomic, physiological, biochemical, and chemotaxonomic findings distinguished strains 4H37-19^T and 3HC-13 from their closely related species and suggested that they represent a novel species within the genus *Corynebacterium*. We propose the name *Corynebacterium poyangense* sp. nov. for strains 4H37-19^T and 3HC-13.

Description of *Corynebacterium poyangense* sp. nov.

Corynebacterium poyangense (po.yang.en'se. N.L. neut. adj. *poyangense*, of or belonging to Poyang Lake from where the type strain was isolated)

Cells are Gram-stain-positive, non-spore-forming, facultatively anaerobic, non-motile and short rods to coccoid (0.2–0.4 × 0.6–0.9 μm). Colonies are creamy whitish, circular colonies with rough edges on TSA at 37°C after 48 h. Cells grow at 15–45°C and pH 6.0–9.0 and in the presence of 0–7.5% (w/vol) NaCl. Optimal growth occurs at 37°C and pH 7.0 and in the presence of 0.5–1.5% (w/vol) NaCl. Cells are positive for acid phosphatase, alkaline phosphatase, esterase (C4), naphthol-AS-BI-phosphohydrolase, trypsin, α-glucosidase, β-galactosidase, β-glucosidase, and β-glucuronidase, but negative for cystine arylamidase, hydrolysis, leucine arylamidase, lipase (C8), N-acetyl-β-glucosaminidase, reduction of nitrates, pyrazinamidase, urease, valine arylamidase, α-chymotrypsin, α-fucosidase, α-galactosidase, α-glucosidase, and α-mannosidase. Cells can assimilate arbutin, esculin ferric citrate, D-fructose, D-glucose, D-maltose, D-mannose, D-ribose, D-trehalose, D-turanose, gentiobiose, gluconate, L-arabinose, and surcose, but not assimilate amygdalin, erythritol, dulcitol, D-adonitol, D-arabinose, D-arabitol, D-cellobiose, D-fucose, D-lyxose, D-melezitose, D-melibiose, D-raffinose, D-tagatose, D-sorbitol, inositol, inulin, mannitol, methyl α-D-glucopyranoside, methyl α-D-mannopyranoside, methyl-βD-xylopyranoside, N-acetylglucosamine, galactose, glycerol, glycogen, lactose, L-arabitol, L-fucose, L-rhamnose, L-sorbose, salicin, starch, xylitol, or xylose. The major fatty acids are $C_{18:1}\omega9c$, $C_{16:0}$, and $C_{18:0}$, while MK-8 (H_4), MK-8(H_2), and MK-9(H_2) are predominant respiratory quinones. The major polar lipids are DPG, PG, PI, PC, and PIM. The major whole cell sugar was arabinose, and the cell wall included mycolic acids. The cell wall peptidoglycan contained *meso*-DAP. The genomic DNA G + C content is 52.5%.

The type strain is 4H37-19^T (= GDMCC 1.1738^T = KACC 21671^T), isolated from the feces of the greater white-fronted geese (*Anser albifrons*) at Poyang Lake, China. The GenBank/EMBL/DDBJ accession numbers for the 16S rRNA gene and genome sequences of strains 4H37-19^T strain 3HC-13 are MN611115 and MN611764 (16S rRNA gene), and CP-046884 and WWCB00000000 (genome), respectively.

Acknowledgements

This work was supported by grants from the National Science and Technology Major Project (2018ZX10301407-002), the Major Science and Project of Jiangxi Province (20201BBG-71010), and the Independent Research Project of State Key Laboratory of Infectious Disease Prevention and Control (2019SKLID311).

We express our sincere gratitude to the Jiangxi Province Department of Forestry for organizing the rescue of migratory birds and sampling. We are also grateful to the staff at Nanchang Center for Disease Prevention and Control who contributed to the sampling.

Conflict of Interest

The authors declare that there are no conflicts of interest.

Ethical Statements

The migratory birds were live captured in Jiangxi province, China. All animals were subjected to non-invasive sampling (feces) and then released. We only collected feces for relevant microbiological studies. The animal welfare practices associated with this study were reviewed and approved by the Jiangxi Province Department of Forestry (No. 20181030).

References

Bauer, A.W., Kirby, W.M., Sherris, J.C., and Turck, M. 1966. Antibiotic susceptibility testing by a standardized single disk method. *Am. J. Clin. Pathol.* **45**, 493–496.

Bernard, K.A. and Funke, G. 2015. *Corynebacterium*. *In* Whitman, W.B., Rainey, F., Kämpfer, P., Trujillo, M., Chun, J., DeVos, P., Hedlund, B., and Dedysh, S. (eds.), Bergey's Manual of Systematics of Archaea and Bacteria, pp. 1–70. John Wiley & Sons, Inc., New York, USA.

Blin, K., Shaw, S., Kloosterman, A.M., Charlop-Powers, Z., van Wezel, G.P., Medema, M.H., and Weber, T. 2021. antiSMASH 6.0: improving cluster detection and comparison capabilities. *Nucleic Acids Res.* **49**, W29–W35.

Boros, Á., Pankovics, P., Simmonds, P., Kiss, T., Phan, T. G., Delwart, E., and Reuter, G. 2018. Genomic analysis of a novel picornavirus from a migratory waterfowl, greater white-fronted goose (*Anser albifrons*). *Arch. Virol.* **163**, 1087–1090.

Braun, M.S., Wang, E., Zimmermann, S., and Wink, M. 2018. *Corynebacterium heidelbergense* sp. nov., isolated from the preen glands of Egyptian geese (*Alopochen aegyptiacus*). *Syst. Appl. Microbiol.* **41**, 564–569.

Braun, M.S., Zimmermann, S., Danner, M., Rashid, H., and Wink, M. 2016. *Corynebacterium uropygiale* sp. nov., isolated from the preen gland of Turkeys (*Meleagris gallopavo*). *Syst. Appl. Microbiol.* **39**, 88–92.

Brettin, T., Davis, J.J., Disz, T., Edwards, R.A., Gerdes, S., Olsen, G.J., Olson, R., Overbeek, R., Parrello, B., Pusch, G.D., *et al.* 2015. *RASTtk*: A modular and extensible implementation of the RAST algorithm for building custom annotation pipelines and annotating batches of genomes. *Sci. Rep.* **5**, 8365.

Busse, H.J., Kleinhagauer, T., Glaeser, S.P., Spergser, J., Kampfer, P., and Ruckert, C. 2019. Classification of three corynebacterial strains isolated from the Northern Bald Ibis (*Geronticus eremita*): proposal of *Corynebacterium choanae* sp. nov., *Corynebacterium pseudopelargi* sp. nov., and *Corynebacterium gerontici* sp. nov. *Int. J. Syst. Evol. Microbiol.* **69**, 2928–2935.

Chun, J., Oren, A., Ventosa, A., Christensen, H., Arahal, D.R., da Costa, M.S., Rooney, A.P., Yi, H., Xu, X.W., De Meyer, S., *et al.* 2018. Proposed minimal standards for the use of genome data for the taxonomy of prokaryotes. *Int. J. Syst. Evol. Microbiol.* **68**, 461–466.

Collins, M.D., Pirouz, T., Goodfellow, M., and Minnikin, D.E. 1977. Distribution of menaquinones in actinomycetes and corynebacteria. *J. Gen. Microbiol.* **100**, 221–230.

Darling, A.E., Tritt, A., Eisen, J.A., and Facciotti, M.T. 2011. Mauve assembly metrics. *Bioinformatics* **27**, 2756–2757.

Fukuda, A., Usui, M., Ushiyama, K., Shrestha, D., Hashimoto, N., Sakata, M.K., Minamoto, T., Yoshida, O., Murakami, K., Tamura, Y., *et al.* 2021. Prevalence of antimicrobial-resistant *Escherichia coli* in migratory greater white-fronted geese (*Anser albifrons*) and their habitat in Miyajimanuma, Japan. *J. Wildl. Dis.* **57**, 954–958.

Guerrant, G.O., Lambert, M.A., and Moss, C.W. 1981. Gas-chromatographic analysis of mycolic acid cleavage products in mycobacteria. *J. Clin. Microbiol.* **13**, 899–907.

Jackman, P. J. H., Pitcher, D. G., Pelczynska, S., and Borman, P. 1987. Classification of corynebacteria associated with endocarditis (group JK) as *Corynebacterium jeikeium* sp. nov. *Syst. Appl. Microbiol.* **9**, 83–90.

Kim, K.R., Kim, K.H., Khan, S.A., Kim, H.M., Han, D.M., and Jeon, C.O. 2021. *Lysobacter arenosi* sp. nov. and *Lysobacter solisilvae* sp. nov. isolated from soil. *J. Microbiol.* **59**, 709–717.

Komagata, K. and Suzuki, K.I. 1988. 4 Lipid and cell-wall analysis in bacterial systematics. *In* Colwell, R.R. and Grigorova, R. (eds.), Methods in Microbiology, pp. 161–207. Academic Press, Cambridge, Messachusetts, USA.

Kumar, S., Stecher, G., Li, M., Knyaz, C., and Tamura, K. 2018. MEGA X: molecular evolutionary genetics analysis across computing platforms. *Mol. Biol. Evol.* **35**, 1547–1549.

Lee, I., Kim, Y.O., Park, S.C., and Chun, J. 2016. OrthoANI: an improved algorithm and software for calculating average nucleotide identity. *Int. J. Syst. Evol. Microbiol.* **66**, 1100–1103.

Li, W., O'Neill, K.R., Haft, D.H., DiCuccio, M., Chetvernin, V., Badretdin, A., Coulouris, G., Chitsaz, F., Derbyshire, M.K., Durkin, A.S., *et al.* 2021. RefSeq: expanding the Prokaryotic Genome Annotation Pipeline reach with protein family model curation. *Nucleic Acids Res.* **49**, D1020–D1028.

Liu, Q., Wu, K., Fan, G., Bai, X., Yang, X., Pan, Y., Cao, L., Song, W., Chen, S., Xiong, Y., *et al.* 2021a. *Corynebacterium anserum* sp. nov., isolated from the faeces of greater white-fronted geese (*Anser albifrons*) at Poyang Lake, PR China. *Int. J. Syst. Evol. Microbiol.* **71**. doi: 10.1099/ijsem.0.004637.

Liu, Q., Xue, L., Wu, K., Fan, G., Bai, X., Yang, X., Cao, L., Sun, H., Song, W., Pan, Y., *et al.* 2021b. *Nanchangia anserum* gen. nov., sp. nov., isolated from feces of greater white-fronted geese (*Anser albifrons*). *Int. J. Syst. Evol. Microbiol.* **71**. doi: 10.1099/ijsem.0.004978.

Ludwig, W., Euzéby, J.P., and Whitman, W.B. 2015. Taxonomic outline of the phylum *Actinobacteria*. *In* Whitman, W.B. (ed.), Bergey's Manual of Systematics of Archaea and Bacteria. pp. 1–4. John Wiley & Sons, Inc., Chichester, United Kingdom.

Luo, C., Rodriguez-R, L.M., and Konstantinidis, K.T. 2014. MyTaxa: an advanced taxonomic classifier for genomic and metagenomic sequences. *Nucleic Acids Res.* **42**, e73.

Meier-Kolthoff, J.P., Carbasse, J.S., Peinado-Olarte, R.L., and Göker, M. 2022. TYGS and LPSN: a database tandem for fast and reliable genome-based classification and nomenclature of prokaryotes. *Nucleic Acids Res.* **50**, D801–D807.

Minnikin, D.E., O'Donnell, A.G., Goodfellow, M., Alderson, G., Athalye, M., Schaal, A., and Parlett, J.H. 1984. An integrated procedure for the extraction of bacterial isoprenoid quinones and polar lipids. *J. Microbiol. Methods* **2**, 233–241.

Na, S.I., Kim, Y.O., Yoon, S.H., Ha, S., Baek, I., and Chun, J. 2018. UBCG: up-to-date bacterial core gene set and pipeline for phylogenomic tree reconstruction. *J. Microbiol.* **56**, 280–285.

Nouioui, I., Carro, L., García-López, M., Meier-Kolthoff, J.P., Woyke, T., Kyrpides, N. C., Pukall, R., Klenk, H.-P., Goodfellow, M., and Göker, M. 2018. Genome-based taxonomic classification of the phylum *Actinobacteria*. *Front. Microbiol.* **9**, 2007.

Oh, Y.J., Kim, J.Y., Jo, H.E., Park, H.K., Lim, S.K., Kwon, M.S., and Choi, H.J. 2020. *Lentibacillus cibarius* sp. nov., isolated from kimchi, a Korean fermented food. *J. Microbiol.* **58**, 387–394.

Oren, A. and Garrity, G.M. 2021. Valid publication of the names of forty-two phyla of prokaryotes. *Int. J. Syst. Evol. Microbiol.* **71**, 3379–3393.

Parte, A.C., Sardà Carbasse, J., Meier-Kolthoff, J.P., Reimer, L.C.,

and Göker, M. 2020. List of prokaryotic names with standing in nomenclature (LPSN) moves to the DSMZ. *Int. J. Syst. Evol. Microbiol.* **70**, 5607–5612.

Price, M.N., Dehal, P.S., and Arkin, A.P. 2010. FastTree 2– approximately maximum-likelihood trees for large alignments. *PLoS ONE* **5**, e9490.

Rossi-Tamisier, M., Benamar, S., Raoult, D., and Fournier, P.E. 2015. Cautionary tale of using 16S rRNA gene sequence similarity values in identification of human-associated bacterial species. *Int. J. Syst. Evol. Microbiol.* **65**, 1929–1934.

Salam, N., Jiao, J.Y., Zhang, X.T., and Li, W.J. 2020. Update on the classification of higher ranks in the phylum *Actinobacteria*. *Int. J. Syst. Evol. Microbiol.* **70**, 1331–1355.

Samuel, M.D., Shadduck, D.J., and Goldberg, D.R. 2005. Avian cholera exposure and carriers in greater white-fronted geese breeding in Alaska, USA. *J. Wildl. Dis.* **41**, 498–502.

Sasser, M. 1990. Identification of bacteria by gas chromatography of cellular fatty acids. MIDI Technical Note 101. MIDI Inc., Newark, Delaware, USA.

Schaeffer, A.B. and Fulton, M.D. 1933. A simplified method of staining endospores. *Science* **77**, 194.

Schumann, P. 2011. 5 - Peptidoglycan structure. *In* Rainey, F. and Oren, A. (eds.), Methods Microbiology, vol. 38, pp. 101–129. Academic Press, London, United Kingdom.

Sharma, N.C., Efstratiou, A., Mokrousov, I., Mutreja, A., Das, B., and Ramamurthy, T. 2019. Diphtheria. *Nat. Rev. Dis. Primers.* **5**, 81.

Sjödén, B., Funke, G., Izquierdo, A., Akervall, E., and Collins, M.D. 1998. Description of some coryneform bacteria isolated from human clinical specimens as *Corynebacterium falsenii* sp. nov. *Int. J. Syst. Bacteriol.* **48**, 69–74.

Walker, B.J., Abeel, T., Shea, T., Priest, M., Abouelliel, A., Sakthikumar, S., Cuomo, C.A., Zeng, Q., Wortman, J., Young, S.K., *et al.* 2014. Pilon: an integrated tool for comprehensive microbial variant detection and genome assembly improvement. *PLoS ONE* **9**, e112963.

Wick, R.R., Judd, L.M., Gorrie, C.L., and Holt, K.E. 2017. Unicycler: resolving bacterial genome assemblies from short and long sequencing reads. *PLoS Comput. Biol.* **13**, e1005595.

Xiang, X., Zhang, F., Fu, R., Yan, S., and Zhou, L. 2019. Significant differences in bacterial and potentially pathogenic communities between sympatric hooded crane and greater white-fronted goose. *Front. Microbiol.* **10**, 163.

Xu, L., Dong, Z., Fang, L., Luo, Y., Wei, Z., Guo, H., Zhang, G., Gu, Y.Q., Coleman-Derr, D., Xia, Q., *et al.* 2019. OrthoVenn2: a web server for whole-genome comparison and annotation of orthologous clusters across multiple species. *Nucleic Acids Res.* **47**, W52–W58.

Yin, Y., Mao, X., Yang, J., Chen, X., Mao, F., and Xu, Y. 2012. dbCAN: a web resource for automated carbohydrate-active enzyme annotation. *Nucleic Acids Res.* **40**, W445–W451.

Yoon, S.H., Ha, S.M., Kwon, S., Lim, J., Kim, Y., Seo, H., and Chun, J. 2017. Introducing EzBioCloud: a taxonomically united database of 16S rRNA gene sequences and whole-genome assemblies. *Int. J. Syst. Evol. Microbiol.* **67**, 1613–1617.

Yoon, S.H., Ha, S.M., Lim, J., Kwon, S., and Chun, J. 2017. A large-scale evaluation of algorithms to calculate average nucleotide identity. *Antonie van Leeuwenhoek* **110**, 1281–1286.

Yu, S., Zheng, B., Chen, Z., and Huo, Y.X. 2021. Metabolic engineering of *Corynebacterium glutamicum* for producing branched chain amino acids. *Microb. Cell Fact.* **20**, 230.

Zhang, H., Yohe, T., Huang, L., Entwistle, S., Wu, P., Yang, Z., Busk, P.K., Xu, Y., and Yin, Y. 2018. dbCAN2: a meta server for automated carbohydrate-active enzyme annotation. *Nucleic Acids Res.* **46**, W95–W101.

Zhu, W., Song, W., Fan, G., Yang, J., Lu, S., Jin, D., Luo, X.L., Pu, J., Chen, H., and Xu, J. 2021. Genomic characterization of a new coronavirus from migratory birds in Jiangxi province of China. *Virol. Sin.* **36**, 1656–1659.

Zhu, W., Zhou, J., Lu, S., Yang, J., Lai, X.H., Jin, D., Pu, J., Huang, Y., Liu, L., Li, Z., and Xu, J. 2022. Isolation and characterization of tick-borne *Roseomonas haemaphysalidis* sp. nov. and rodent-borne *Roseomonas marmotae* sp. nov. *J. Microbiol.* **60**, 137–146.